Available online at www.CivileJournal.org

# Civil Engineering Journal

(E-ISSN: 2476-3055; ISSN: 2676-6957)

Vol. 11, No. 01, January, 2025

# On the Use of a Confined Sand Cell to Dampen Induced Machine Vibration in a Stabilized Clay Numerical Study

Engy M. Kassem [1*], Waseim Azzam [2], Mohamed Elsiragy [3]

[1] *Department of Civil Engineering, Mansoura Higher Institute of Engineering and Technology, Mansoura, Egypt.*

[2] *Department of Structural Engineering, Faculty of Engineering, Tanta University, Tanta, Egypt.*

[3] *Department of Civil Engineering, Faculty of Engineering, October 6 University, Cairo, Egypt.*

Received 04 June 2024; Revised 17 December 2024; Accepted 22 December 2024; Published 01 January 2025

**Abstract**

Environmental vibrations produced often by industrial and construction processes can affect adjacent soils and structures, sometimes resulting in foundation failure and structural damage. The application of confined cells under foundations as a mitigation technique against dynamic sources, such as generators, is investigated in this study. Numerical models were developed using Plaxis 3D software to simulate the effect of a vibrating source on a circular footing, both with and without confined cells filled with sand soil at varying depths and diameters. In these cells, the soil modeling considered compaction loads typical in actual construction conditions. Results indicate that placing a minimum-diameter cell closer to the foundation with adequate penetration depth can significantly enhance dynamic response and reduce subgrade deformation. The effectiveness of confined soil in minimizing displacement amplitude in the foundation is evaluated, revealing an impressive 86% reduction with specific cell dimensions (Hc/D = 0.50 and Dc/D = 1.15). Moreover, peak particle velocity and excess pore water pressure at monitored points in the surrounding environment experience reductions of 62% and 87%, respectively, demonstrating substantial vibration attenuation. The study does effectively highlight the novelty of the confined sand cell approach, positioning it as a more targeted, efficient, and cost-effective alternative to existing methods, especially for conditions where large-scale, deep vibrations are a concern.

*Keywords:* Circular Footing; Dynamic Response; Compaction Effects; Clay Soil; Confined Sand Soil; Plaxis 3D.

## 1. Introduction

In challenging environments, various sources, such as machinery, construction activities, seismic events, and vehicular traffic, can induce vibrations and dynamic responses that pose serious threats to structures and their foundations. These dynamic motions propagate swiftly through the soil, impacting not only the foundations but also the superstructures and surrounding soil. Soil instability triggered by these dynamics can result in significant ground movements, including differential settlement, leading to structural damage. Often, the initial cause of such issues stems from the unfavorable response of the soil-foundation system to dynamic pressures.

Vibration and shock originating from machinery, including vibrating, rotating, reciprocating, and striking equipment, play a significant role in this scenario. These vibrations and shocks are transmitted into the soil and its support systems. Unbalanced rotating machinery generates centrifugal forces, contributing to random and steady-state

* Corresponding author: engengy90@gmail.com; eqasem@mca.edu.eg

http://dx.doi.org/10.28991/CEJ-2025-011-01-018

vibrations. Common sources of such vibrations and shocks include machinery that produces pulses or impacts, such as centrifugal pumps, compressors, impact testers, injection molding machines, forging presses, and hammers.

The impact of using a skirted foundation system to enhance the resilience of the superstructure under earthquake loading and improve the deformation properties of the supporting soil was examined by Azzam [1]. According to the results, installing skirts on either side of the foundation improves the kinematic stiffness of the supporting subgrade by reducing the liquefaction potential inside the confined block and enhancing the densification impact. Additionally, the skirts increase the building's rigidity during an earthquake and significantly reduce the building's acceleration and lateral displacement. Using the Plaxis dynamic program, Azzam [2] examined the use of a confined cell beneath foundations to reduce and manage dynamic effects on sandy subgrades. The results demonstrated that the dynamic response enhanced, and the overall subgrade deformation reduced when the cell with a minimal diameter was installed closer to the foundation with adequate penetration depth.

The behavior of a machine foundation supported by rigid inclusions was examined by Khalil [3]. The behavior of machine foundations supported by piles, shallow foundations, and rigid inclusions is examined in this work. The loose-to-medium-sized sand in the soil profile chosen for analysis becomes more rigid as depth increases. The analysis findings show that, in contrast to the other two systems, rigid inclusions respond more steadily and have less dynamic displacement. The dynamic properties and reinforcing mechanism of silty soil enhanced by regenerated fiber polymer were investigated by Liu et al. [4]. They examined the microscopic processes and dynamic properties of roadbed silt treated with recycled fiber polymer using dynamic triaxial testing and scanning electron microscopy (SEM) techniques. The results show that the fiber-modified soil sample has the highest dynamic strength, dynamic elastic modulus, and lowest damage at a fiber content of 0.2%. It also has the best resilience to dynamic loads.

The performance of shallow footing under machine foundation stresses was investigated experimentally by Ekal & AbidAwn [5] to determine the optimal number of reinforcement layers using geogrid under a square foundation. Based on the results, one layer was the optimal number of layers at a frequency of 10 Hz. The optimal number of layers was four at a frequency of 15 Hz. The more layers there are, the lower the ratio of settlement.

Tang & Chen [6] examined the dynamic response of a deep-water long-span cable-stayed bridge under the combined action of earthquakes and waves. This study develops a model of a specific deep-water long-span cable-stayed bridge using the finite element method. The findings show that the presence of water enhances the structure's dynamic response to seismic activity, with a maximum increase in structural shear force of 71.57%. The internal force response amplitude of the main tower and auxiliary piers under the combined action is increased by roughly 10% to 12% in comparison to the effect of an earthquake alone. Kennedy [7] used cyclic direct simple shear laboratory measurements to examine the impact of confining pressure on the small-strain shear modulus and damping ratio of sandy soil. The findings demonstrated that the small-strain shear modulus (Gmax) displayed pressure-sensitive behavior, increasing considerably with increasing confining pressure. On the other hand, it was discovered that as confining pressure increased, the maximum damping ratio (Dmax) gradually decreased.

Akpan et al. [8] concentrated on showcasing notable research in this field and demonstrating the potential of artificial neural networks in dynamic response investigations of machine tool foundations. ANN is capable of navigating the search modules and presenting a large number of solutions. Crucially, it includes multiple processing layers for refinement and can accept a large number of inputs, making it a clear practical solution for challenging, complicated engineering problems like machine tool foundation issues. Bazoobandi et al. [9] investigated the potential of surface trenches filled with a mixture of rubber crumb and sand to lessen industrial foundation vibrations. Determining the effect of trench dimensions on insulation levels was the main objective of the study. According to the findings, trench depth and length significantly influenced the result, but thickness had no noticeable impact.

This research introduces a novel approach using confined sand cells to mitigate machine disturbances, comparing favorably to existing vibration isolation techniques as a lateral confinement instrument. This research delved into understanding the behavior of partially confined sand soil within cells using the Finite Element Method (FEM) in Plaxis Dynamic Version 2020 in clay soil. The primary aim was to mitigate dynamic disturbances caused by vibrating sources through the use of confined sand cells beneath foundations and to examine the impact of increasing clay subgrade stiffness. The study explored how compacting the sand layer inside the cells with specific loads affects the sand's behavior. The technique employed proved successful in isolating vibrations from various sources of excitation. A series of numerical analyses were conducted to explore the compaction effect on the behavior of sand soil within the cell, evaluating the suitability of this method for modeling soil compaction in dynamic response. Additionally, the critical and adverse locations of confined sand cells were analyzed relative to the surrounding clay soil. The flowchart demonstrating the research approach is shown in Figure 1.

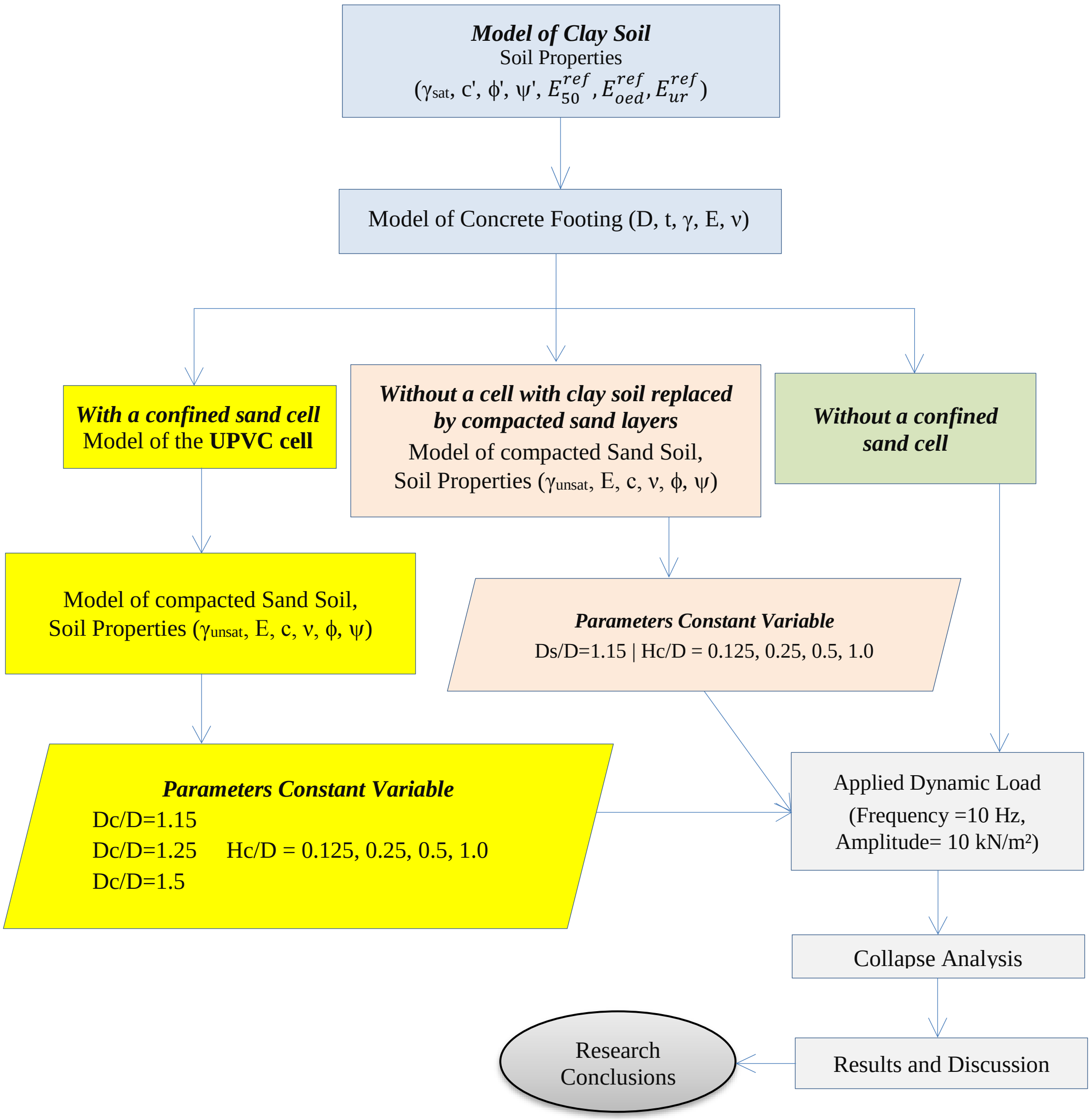


**Figure 1. Flowchart for study methodology**

## 2. Numerical Modelling

The focus of this study revolves around a generator-like vibrating source featuring a circular reinforced concrete foundation, situated atop a layer of medium clay, with the option of incorporating a confined sand cell (refer to Figure 2). To capture the physical damping effects, Rayleigh damping is employed.

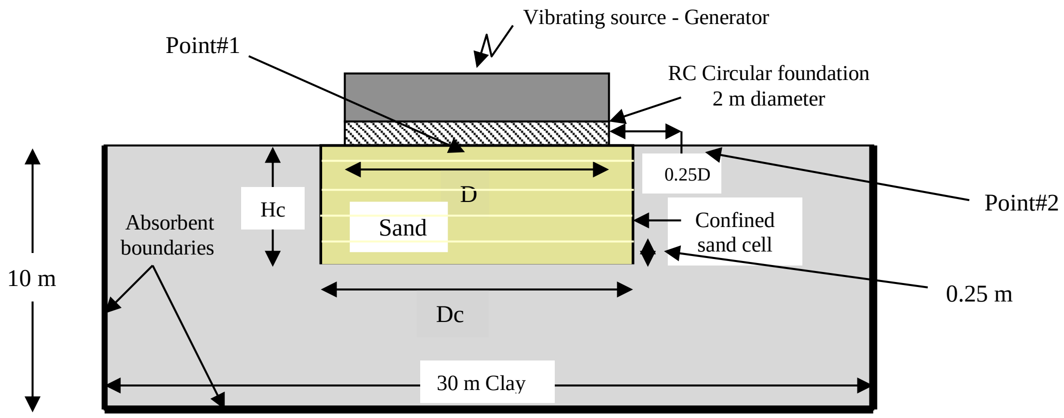


**Figure 2. Diagrammatic representation of the model and problem being studied**

Mesh generation is facilitated by the program, with particular refinement in the vicinity of the footing. The subsoil consists of a 10-meter-thick layer of clay, treated as a hardening soil model for dynamic analysis. The clay's properties ($\gamma_{sat}$ = 17.5 kN/m$^3$, c' = 10, ϕ' = 25, ψ'= 0, $E_{50}^{ref}$ = 1.65 MPa, $E_{oed}^{ref}$ = 1.65 MPa and $E_{ur}^{ref}$ = 5.4 MPa) are as specified by Likitlersuang et al. [10].

To mitigate potential disturbances from reflections, the model boundaries are positioned sufficiently far from the area of interest. Despite implementing absorbent boundaries to minimize unwanted reflections, residual effects persist, necessitating boundaries set much farther than in static analyses. Therefore, Rayleigh damping is applied at the vertical boundaries, with the damping ratio (ξ) set to 5% for coefficients α and β, as automatically determined by the program and specified in the manual [11].

The plastic behavior of the soil is characterized by Rayleigh damping throughout the analytical process. Considering excess pore water pressure, the groundwater table is assumed to be at the ground surface, resulting in undrained soil conditions.

The vibrating source consists of a generator mounted on a reinforced concrete footing with dimensions of 0.50 meters thick and 2 meters in diameter. These vibrations with a frequency of 10 Hz and an amplitude of 10 kN/m$^2$ (Figure 2) propagate through the soil. The oscillations are accompanied by the weight of footing and an assumed generator weight of 8 kN/m$^2$. It is modeled as a uniformly distributed load, as specified in the manual.

The elastic concrete footing is simulated as a plate element, characterized by properties (E = 2.2e7 kN/m$^2$, γ = 25 kN/m$^2$, and Poisson's ratio ν = 0.15).

Constructed from unplasticized polyvinyl chloride (UPVC), the confining cell varies in depth and diameter, with a uniform thickness of 4 mm. The mechanical characteristics of the tested cell, detailed in Table 1 and in accordance with Azzam [2], depend on factors such as temperature, wall thickness, homogeneity, and loading rate.

**Table 1. Properties of the utilized UPVC cell**

| Properties | Values |
|---|---|
| Specific gravity | 1.4 |
| Tensile modulus | 28 $10^3$ kPa |
| Tensile strength | 55 $10^3$ kPa |
| Max. hydraulic pressure for 1 h at 23ºc | 23, Bar |
| Water absorption at 100ºc for 24 h | 4 mg/cm$^3$ |

Containing dense sand soil, the cell adopts the Mohr-Coulomb soil model for dynamic analysis, with the sand's properties ($\gamma_{unsat}$ = 19 kN/m$^3$, E = 65Mpa, c = 1, ν = 0.3, ϕ = 38º, ψ= 8) sourced from Allawi & Mohammed [12].

The models are run using different cell depths (Hc/D) and diameters (Dc/D), where Hc denotes the cell height, D represents the footing diameter, and Dc indicates the cell diameter. The study examines (Hc/D) ratios of 0.125, 0.25, 0.5, and 1.0, as well as (Dc/D) ratios ranging from 1.15 to 1.50, as outlined in Table 2. The cell is modeled as a plate element, with an interface element utilized between the soil and the cell. Monitoring within the confined area includes point #1, located at the foundation level, and point #2, positioned at a distance of 0.25D from the footing face outside the confined area, in the free field. These measurements are used to assess performance during dynamic stimulation.

**Table 2. Schematic of the numerical analysis for clay, both reinforced and unreinforced, under dynamic loading**

| Series | Constant Parameters | Variable Parameters |
|---|---|---|
| 1 | Unreinforced Clay Soil | ------------------ |
| 2 | Dc/D=1.15 | Hc/D = 0.125, 0.25, 0.5, 1.0 |
| 3 | Dc/D=1.25 | Hc/D = 0.125, 0.25, 0.5, 1.0 |
| 4 | Dc/D=1.5 | Hc/D = 0.125, 0.25, 0.5, 1.0 |
| 5 | Clay Soil without Cell & Ds/D=1.15 | Hs/D = 0.125, 0.25, 0.5, 1.0 |
| 6 | Unreinforced Clay Soil, Dc/D=1.15 & Hc/D=0.125, 0.25, 0.5, 1.0 | Dynamic Stresses = -1, -2, -3 kN/m$^2$ |
| 7 | Unreinforced Clay Soil, Dc/D=1.15 & Hc/D=0.125, 0.25, 0.5, 1.0 | Amplitude = 10, 15, 20 |

Ds is the diameter of sand soil, and Hs is the depth of sand soil.

## 3. The Finite Element Model's Validation

According to existing literature, the effectiveness of finite element models employing various vibration isolation techniques has been established. However, no experimental or analytical results from the literature were found for comparison regarding the proposed confined sand cell beneath the foundation under dynamic loads. Instead, validation was conducted using the experimental findings of Basha et al. [13], who investigated the use of a sand cushion to stabilize a peat layer, considering dynamic compaction response as a method for vibration isolation. The model was validated by directly comparing it with the results of full-scale field experimental tests conducted by Basha et al. [13], where all model parameters were derived from their research. Basha et al. [13] performed plate loading tests (PLTs) at the studied road location using a circular steel plate with a diameter of 0.60 m on a 0.50 m compacted subgrade layer, both with and without reinforcement. Figure 3 illustrates the parameters tested. Figure 3-a shows the load test for the standard scenario where the plate load is directly above the fill without stabilization, while Figure 3-b demonstrates the application of a 0.50 m thick sand layer compacted in two 250 mm layers, serving as a sand cushion. Each layer was compacted thoroughly to achieve maximum dry density, following specifications provided by Basha et al. [13].

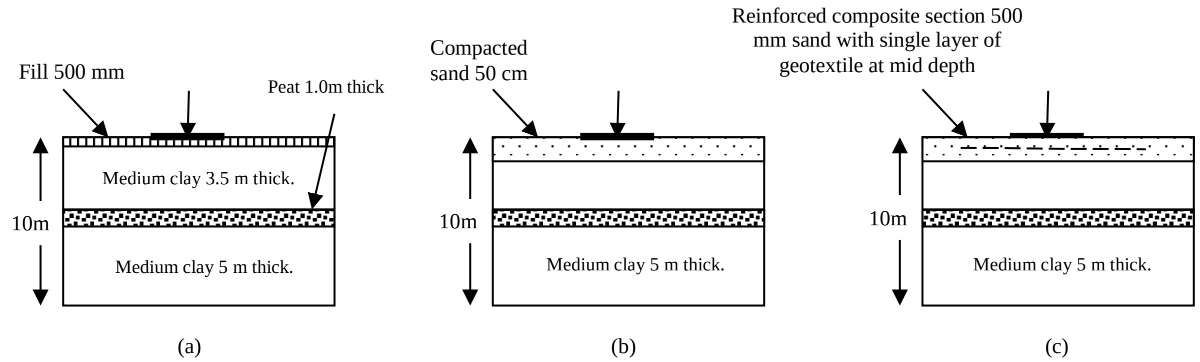


**Figure 3. Plate load tests for various field cases, according to Basha et al. [13]**

The excitation source was dynamically loaded by the site's compaction equipment repeatedly. In the analysis, ten cycles were considered with an applied load of 25 kN/m$^2$ at a frequency of 39 Hz and a time interval of two seconds. This implies that during simulated load cycles, ten of the twenty phases in the simulation were active, while the remaining ten were inactive.

The numerical calculations and the field data show a high degree of consistency, both following the same trend, as seen in Figures 4 and 5. Consequently, it was concluded that the computer program used for this research could be applied for the suggested studies, as the adopted Plaxis dynamic version can effectively predict the behaviour of a foundation on a confined sand cell under a vibration source.

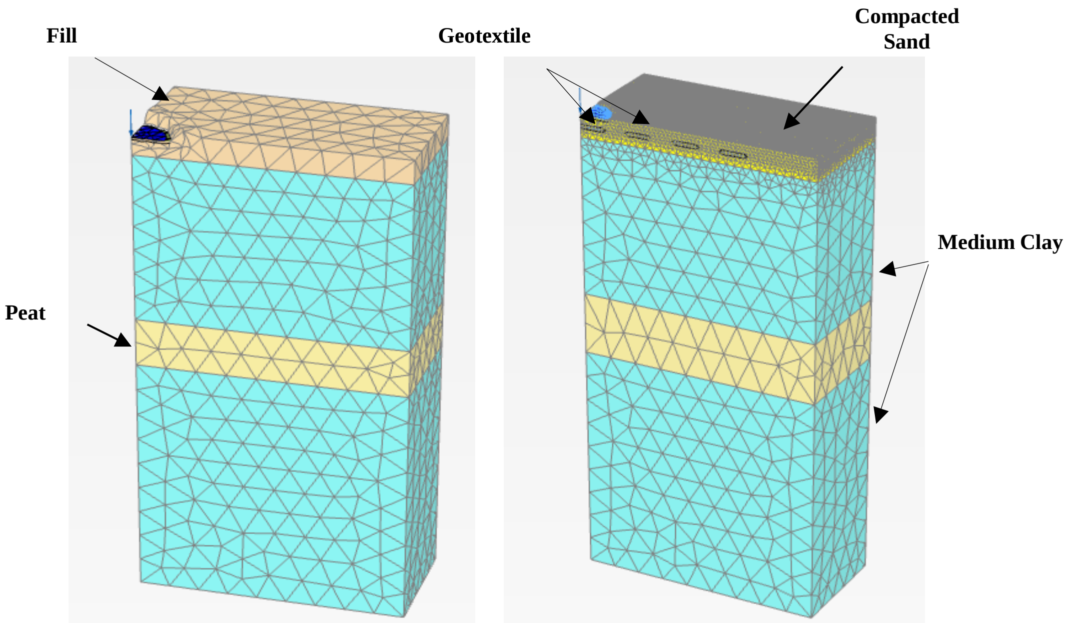


**Figure 4. Plaxis 3D models used for validation**

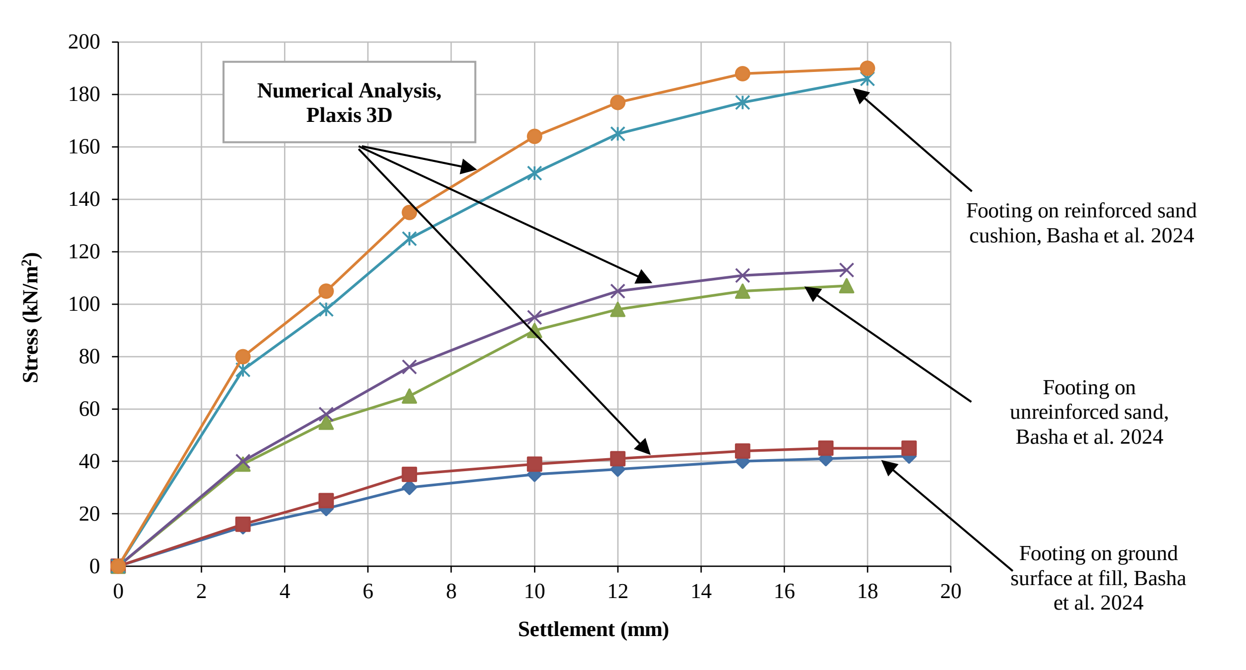


**Figure 5. Stress settlement-curve comparison between field test data (Basha et al. 2024) [13] and numerical outcomes (Plaxis 3D) for various scenarios**

## 4. Explanation of Compaction Loadings and Staged Construction using Plaxis 3D

Compaction loading refers to the process of applying loads to the soil to simulate the effect of compaction or consolidation, typically during construction or embankment formation. The objective is to achieve a more dense and stable soil structure by compacting it, which in turn changes the soil's stress-strain behavior.

Dynamic numerical models were executed for the system with and without a confined sand cell, varying parameters such as cell depths and diameters. The computational process traversed multiple phases, contingent upon the depth of the cell. The soil modeling considered compaction loads typical of actual construction conditions, employing plastic calculation techniques within Plaxis 3D.

To simulate the segmental compaction load in the sand soil within the cell, the construction process unfolds as follows:

***Stage 1:*** The clay soil is modeled using the Plaxis 3D program. Subsequently, the soil is excavated in the area designated for placing the confined sand cell beneath the foundation. The cell is then positioned in the excavated area.

***Stage 2:*** The first layer of sandy soil, with a thickness of 0.25 meters, is placed in the excavated area and inside the cell.

***Stage 3:*** A compaction load is applied to the sandy soil inside the cell.

***Stage 4:*** Successive layers of sandy soil are placed inside the confined cell, with each layer being compacted individually before the next layer is added until the ground surface is reached. Compaction loads are uniformly applied atop each layer and promptly removed upon the placement of the subsequent volume of sandy soil, as stated by Won & Langcuyan [14], Mirmoradi & Ehrlich [15], Cui et al. [16] and Mirmoradi & Ehrlich [17].

***Stage 5:*** After construction is completed, the compaction loads are removed, and the concrete footing is installed. Subsequently, static loads are applied to represent the weight of the generator. Additionally, a uniform load of 10 kPa is applied on top of the concrete footing to simulate surcharge loads.

***Stage 6:*** Finally, the last phase of construction aligns with the operational phase of the generator. During this stage, a vertical harmonic load with a frequency of 10 Hz and an amplitude of 10 kN/m² is applied to simulate the vibrations transmitted by the generator. All parameters in the dynamic analysis start from zero, with the final two stages focusing on dynamic calculations.

Figure 6 illustrates the Plaxis 3D model developed for this study, showcasing the specific arrangement of sand soil within the cell and the staggered application of compaction loadings. Furthermore, Figure 7 shows the modeling process from the start of excavation to loading in steps within the PLAXIS software.

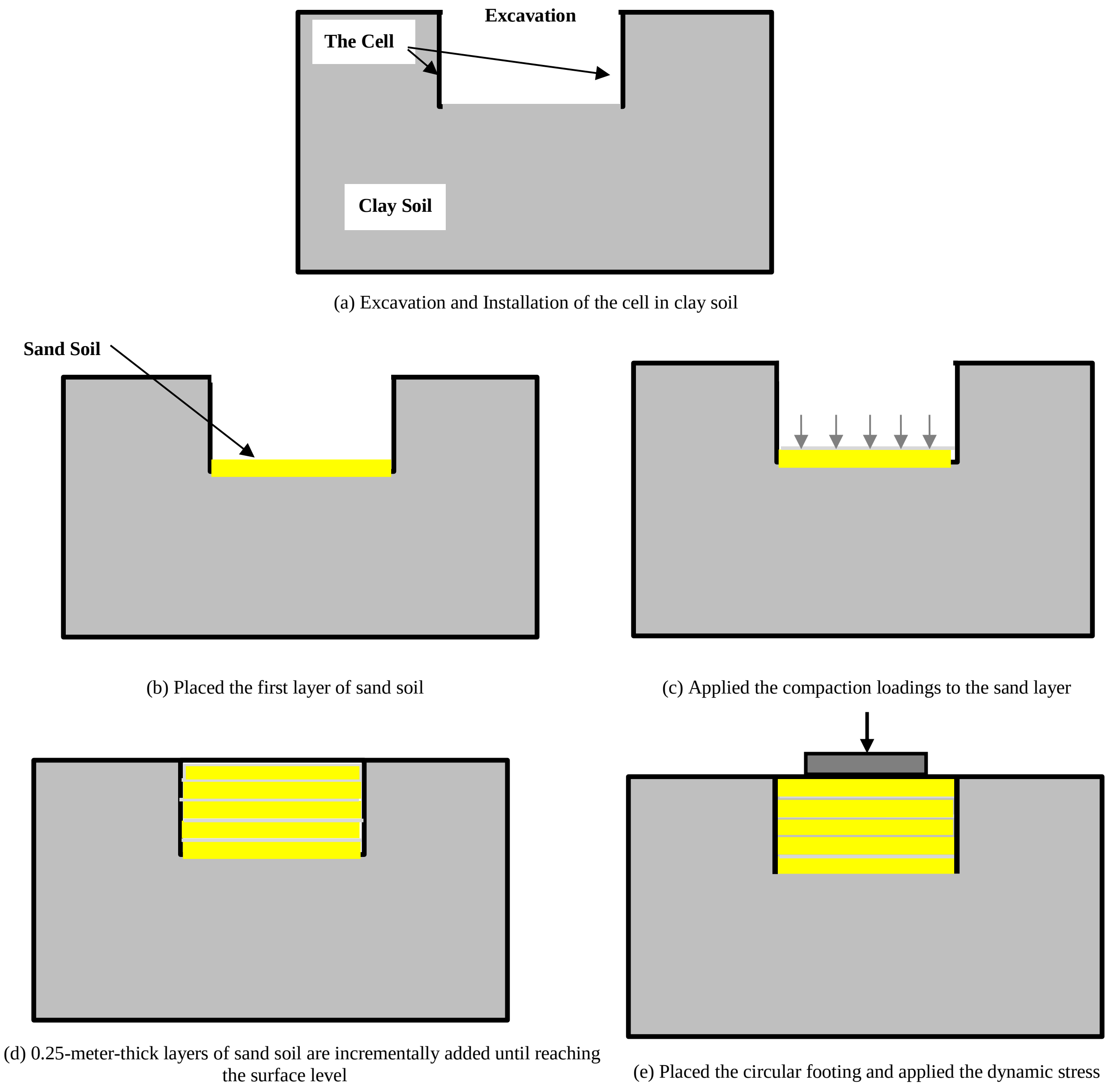


**Figure 6. Installation steps for simulation of compaction in the replaced sand layer under dynamic stresses in Plaxis 3D**

Woods [18] introduced the amplitude reduction factor (Am) as a measure of the screening effectiveness of a confined cell acting as a barrier. Given the variability observed in different studies, using the average amplitude reduction factor (Am) provides a comprehensive measure of isolation effectiveness. A lower Am value indicates a stronger screening effect.

The amplitude reduction ratio, denoted as Am, is calculated as the ratio of the amplitude observed with a confined sand cell to that observed without it. This metric is used to assess the efficacy of the cell. Results are typically reported in terms of amplitude reduction ratios, which allow for the evaluation of system effectiveness based on observed displacements, velocities, or accelerations at points #1 and #2 normalized to the peak particle displacement after the cell is executed.

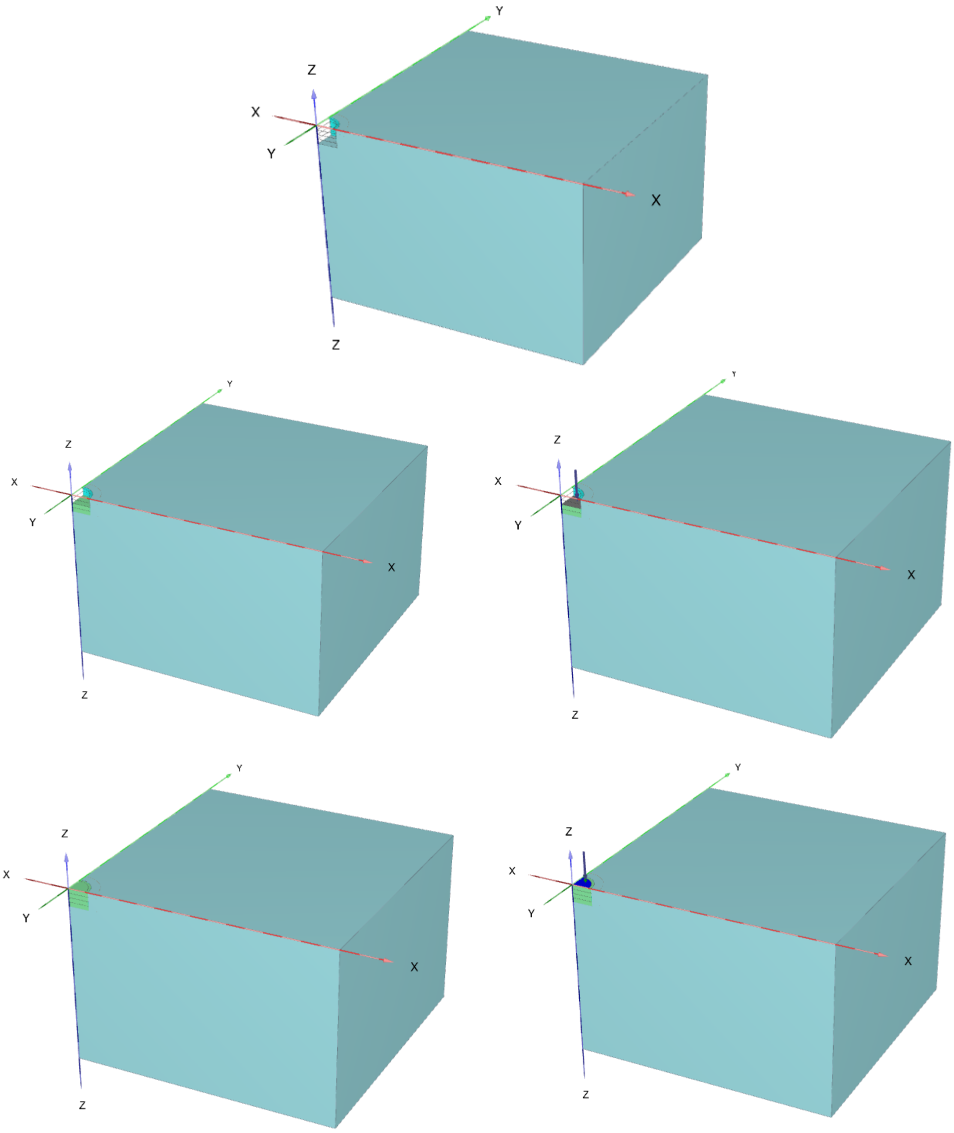


**Figure 7. The model created within the PLAXIS software**

## 5. Results and Discussion

### 5.1. Effect of the Cell on Foundation Subgrade Behaviour

The propagation of body waves from any vibrating source typically expands radially outward along hemispherical wave fronts, while Rayleigh waves follow cylindrical wave fronts. The presence of a confined sand cell introduces a barrier effect, altering the propagation of waves from downward to radial when employed as a vertical barrier around the foundation. Such a confined sand cell is recognized as providing active screening or isolation when positioned beneath the foundation.

By placing the confined cell or barrier, a screening effect is achieved due to a significant increase in subgrade stiffness during dynamic loading. This alteration in the subgrade's deformation properties leads to noticeable changes, allowing for gradual densification of the subgrade during the loading stages. Within the confined subgrade, progressive densification occurs, effectively controlling both vertical and horizontal displacements induced by dynamic effects. Notably, the confined sand cell demonstrates effectiveness in controlling subgrade displacement induced by vibration sources compared to a normal footing without a cell.

Observations reveal that the confined sand cell acts as a vertical barrier, confining the subgrade and preventing heave along each side of the footing at the surface. Additionally, the compacted sand layers within the cell prevent footing punching compared to when no confined sand cell is present. Furthermore, significant lateral contraction resulting from cell installation prevents lateral spreading associated with dynamic excitation below the foundation, thereby preventing soil flow outside to the free field, as stated by Azzam [2].

Overall, the presence of the cell alters the direction of subgrade displacement, dissipating below the limited area with no discernible deformation seen next to the cell. This underscores how the employed cell reduces foundation displacement during loading stages, as reported by Azzam [2], as seen in Figure 8.

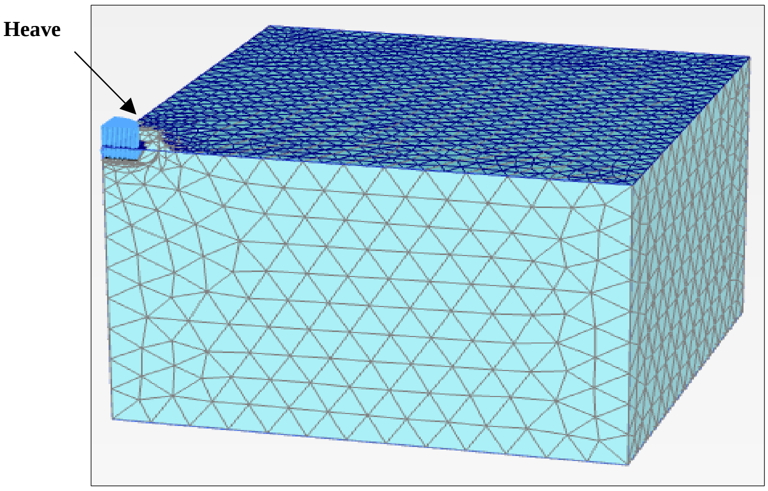


(a) Without confined sand cell

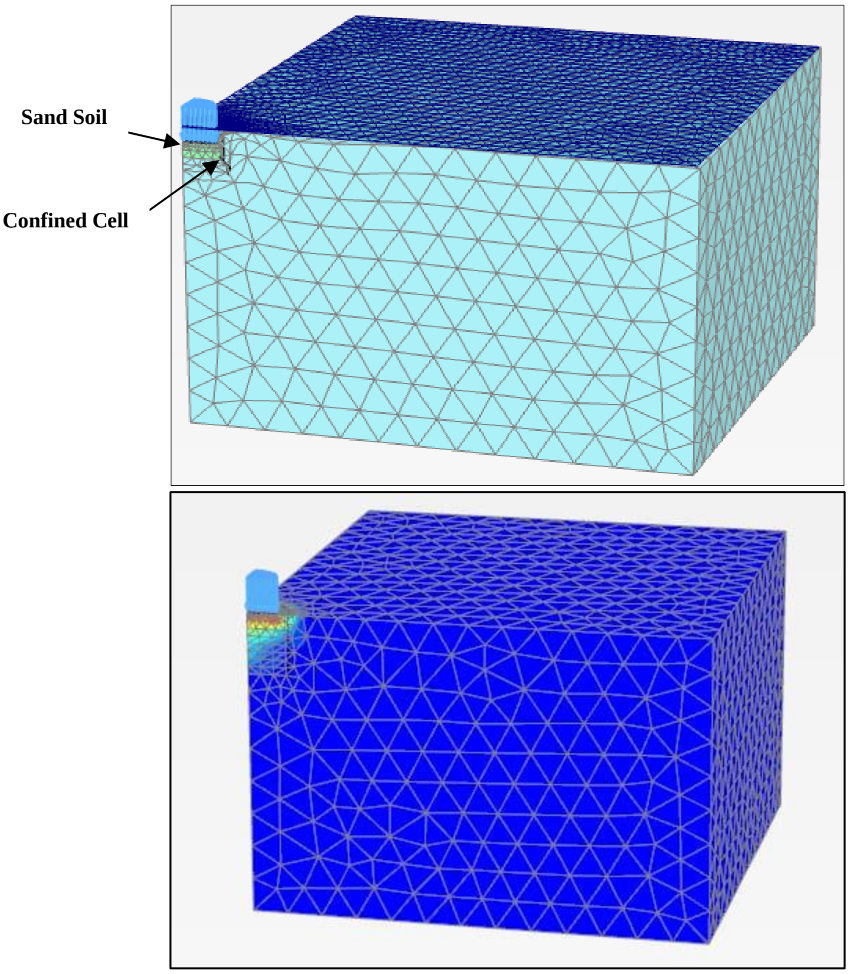


(b) With confined sand cell

**Figure 8. The footing's total displacement vectors under dynamic action, with and without cell**

In cases where no cell is present, footing displacement increases over time. However, the introduction of a cell significantly reduces total foundation displacement, up to 86% for specific cell geometries (Hc/D = 0.50 and Dc/D = 1.15). The densification impact of the cell leads to increased subgrade shear strength by acting as both a vertical barrier and a reinforcing element.

## 5.2. Effect of Depth and Diameter of Cell

Figure 9 illustrates significant differences in overall displacement amplitudes for both footings with and without a cell barrier at points #1 and #2, allowing for an assessment of the barrier's impact on vibration control. Generally, increasing the depth of the cell correlates with greater reductions in all amplitudes. However, it is evident from Azzam

[1] that the decrease in displacement amplitude reduction becomes less pronounced as the cell depth increases. To achieve substantial isolation effects, constructing the cell with adequate embedding depth and a diameter close to that of the footing is crucial. Analysis of Figure 9 indicates that extending the cell penetration beyond a certain threshold (Hc/D = 0.50) does not provide additional benefits, consistent with findings by Azzam [2]. Beyond this ratio, there is a consistent reduction in amplitude, suggesting minimal additional impact. Installing a cell with a depth less than 0.5 times the footing diameter results in a noticeable decrease in the reduction factor (Am), indicating that shallow cells only partially confine the soil (Hc/D < 0.50). Both the location of the monitored point and the depth of the cell influence the maximum improvement in the reduction factor. Effective screening occurs when the cell is placed near the footing with sufficient embedding depth and reduced diameter. A reduction of approximately 13% at point #1 can be achieved with a cell geometry of Hc/D = 0.50 and Dc/D = 1.15. Similarly, a 10% reduction is observed at point #2 in the free field outside the confined cell. This highlights the cell barrier's capability to isolate and mitigate displacements induced by vibration sources.

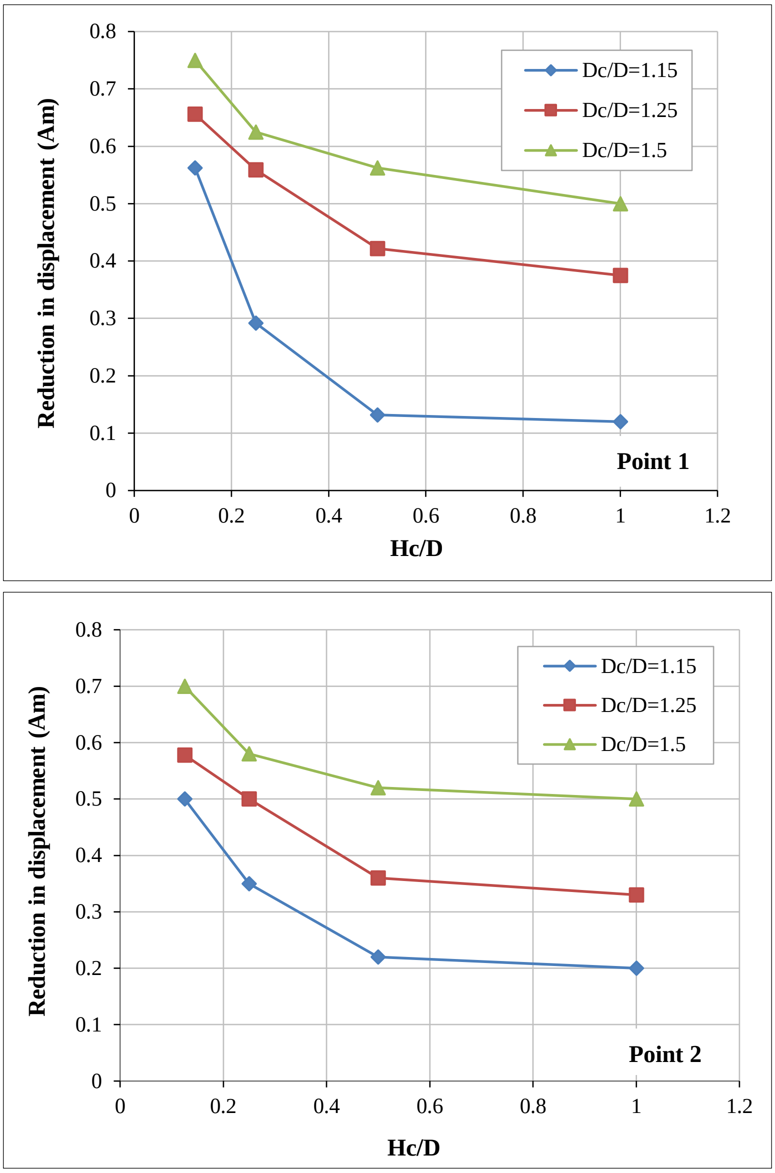


**Figure 9. The variation of Am factor with normalized cell depth for monitored points #1 and #2**

The effect of cell diameter on points #1 and #2 is examined in Figure 10, revealing that the amplitude reduction factor increases with larger cell diameters. At a cell depth of Dc = 1.5 times the footing diameter and Hc/D = 0.50, this factor reaches 56%, but it diminishes to 13% for a normalized cell depth of Dc = 1.15 times the footing diameter at point #1. This reaffirms the beneficial effects of positioning the cell with a diameter close to the footing, creating a sand confinement condition that restricts the propagation of vibrations into the surrounding clay soil.

This confinement plays a crucial role in controlling the lateral spreading induced by vibrations beneath the foundation. When screening devices such as the selected confined sand cell are positioned near the vibration source, it is termed active screening or active isolation. By employing barriers like these, surface waves can be effectively intercepted, scattered, and diffracted, thus attenuating vibrations.

It can be said that the interplay between cell depth and diameter in the response of footing, particularly when the cell is positioned at the footing's base, is pivotal for vibration control and isolation. Primarily, the depth of the cell determines the degree of soil confinement and restraint. Deeper cells offer increased anchorage and confinement, effectively curtailing the lateral spread of vibrations beneath the foundation. This confinement effect is particularly pronounced when the cell is situated at the bottom of the footing, directly engaging with the soil layers through which vibrations propagate. Secondly, the diameter of the cell dictates its coverage area and interaction with the surrounding soil. Larger diameters afford broader coverage and more extensive interaction, enhancing the efficacy of vibration reduction. Placed at the footing's base, a larger cell diameter facilitates the even distribution of confinement effects across the soil, thereby diminishing the transmission of vibrations to neighboring regions. Consequently, the combined influence of cell depth and diameter, especially when positioned beneath the footing, significantly enhances vibration control and isolation. This synergy provides sufficient confinement and coverage to effectively mitigate the spread of vibrations through the soil.

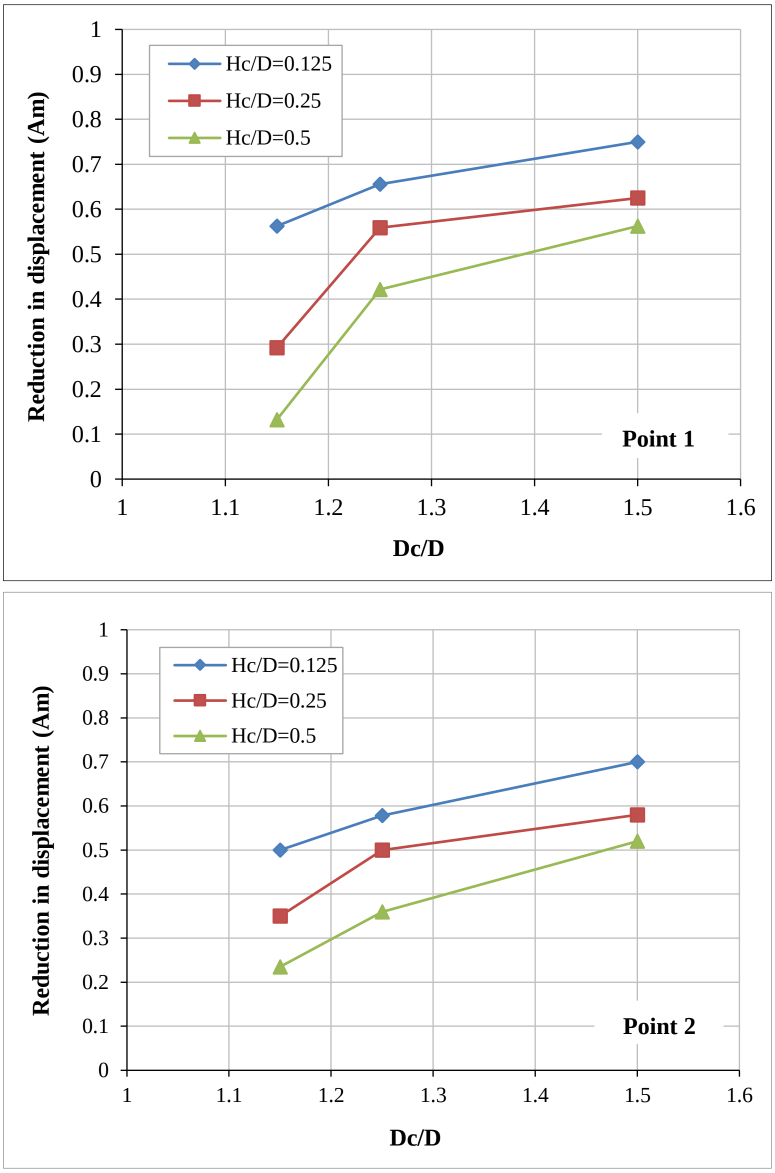


**Figure 10. Variation of Am factor with normalized cell diameter for monitored points #1 and #2**

### 5.3. The Impact of the Cell on Peak Particle Velocity

Alternatively, an additional analysis was conducted to assess the effect of the confined cell on peak particle velocity data at point #2, situated in the open field beyond the confined cell. Figure 11 depicts the variation in peak particle velocity based on the presence of the cell within the footing subgrade. It highlights that installing the cell with a minimal diameter and appropriate depth results in a substantial reduction in peak particle velocity at point #2.

Specifically, the reduction in peak particle velocity reaches 59% compared to its initial value without a cell, with a cell geometry of Hc/D = 0.25 and Dc/D = 1.15. This reduction percentage increases to 62% at Hc/D = 0.50 and Dc/D = 1.15. These observations underscore the cell's ability to obstruct surface waves, consistently decreasing peak soil particle velocity in the open field. The employed cell effectively mitigates vibrations transmitted to the surrounding soil, as demonstrated by the significant decrease in velocity at point #2 in the open field.

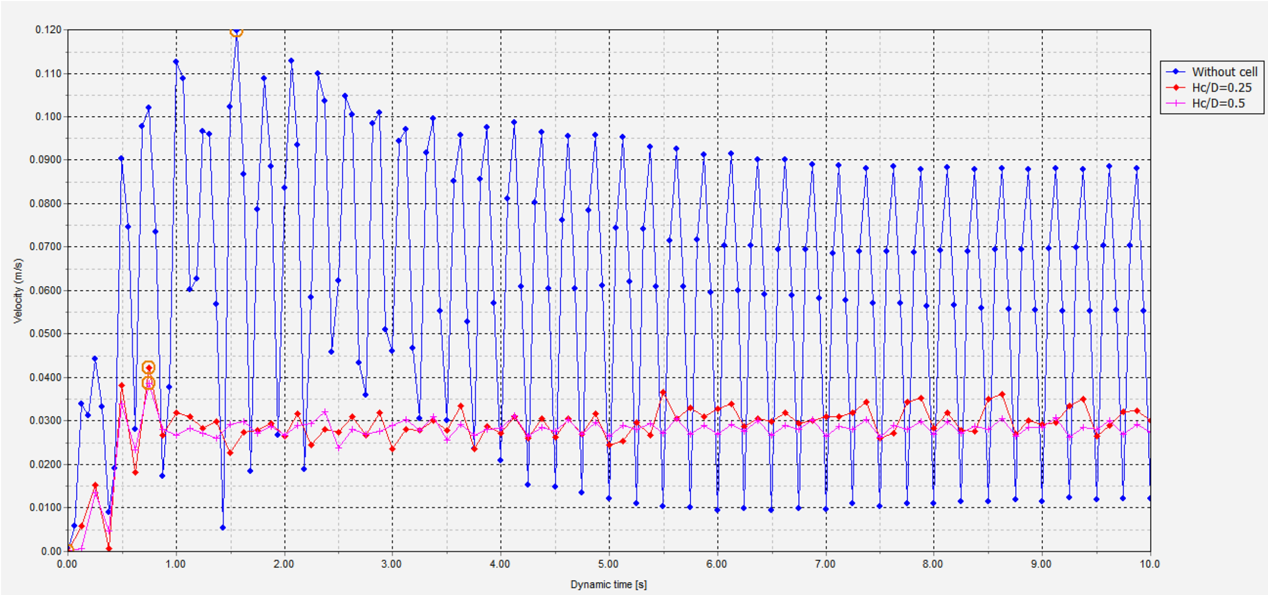


**Figure 11. Time vs. velocity curve for point #2 at Dc/D = 1.15**

## 5.4. The Impact of the Cell on Excess Pore Water Pressure

Figure 12 illustrates the relationship between reductions in excess pore water pressure over time at various depths of the confined sand cell, focusing on its influence on induced pore water pressure in the adjacent soil at free field point #2. The cell is designed to regulate excess pore water pressure generated by the vibration source, effectively preventing its dissipation into the surrounding environment. A comparison between situations with and without cells shows a decrease in excess pore pressure as the cell depth increases, maintaining a constant cell diameter (Dc/D = 1.15). At depths of Hc/D = 0.25 and 0.50, excess pore water pressure decreases by 63% to 87% compared to its initial value in the absence of a cell.

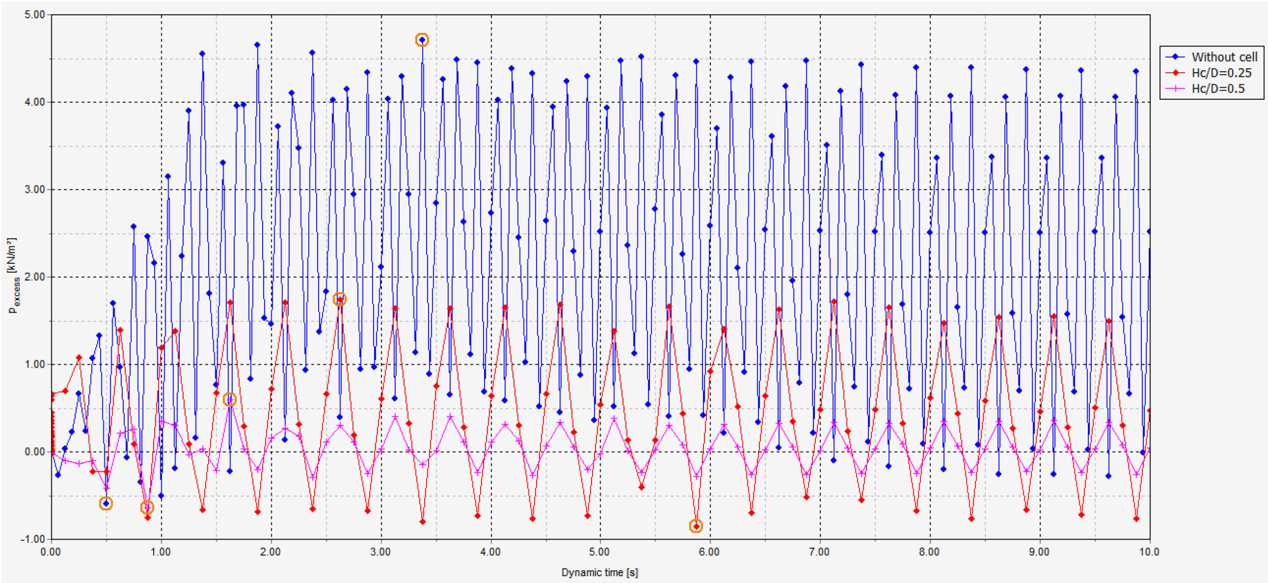


**Figure 12. Time vs. excess pore water pressure curve for point #2 at Dc/D = 1.15**

Additionally, it is observed that with a small cell diameter and adequate embedding depth, the migration of pore water pressure is confined within the cell's boundaries. As a result, excess pore water pressure accumulates solely beneath this zone, demonstrating that the confined cell effectively mitigates the induced excess pore water pressure from the vibration source to the surrounding soil.

This finding underscores the effectiveness of the confined cell in absorbing disturbances caused by the densification effect. Figure 12 further highlights the capability of the confined zones to control and limit the lateral migration of pore water pressure beyond the cell boundary at point #2. The effect of the confined sand cell on excess pore water pressure is consistent with findings from previous studies, as reported by Azzam [2] and Aminfar et al. [19].

Comparative analysis between cases with and without cells aligns with research by Azzam [2], demonstrating a decrease in excess pore pressure with increasing cell depth at a constant diameter. This reduction in excess pore water pressure has been observed to range from 63% to 80% compared to the initial value without a cell, as reported by Finno & Zapata-Medina [20], highlighting the effectiveness of the confined cell in mitigating excess pore water pressure from the vibration source to the surrounding soil.

The findings also support the concept of the confined cell's ability to absorb disturbances resulting from the densification effect, in line with research by Akan & Sert [21].

### 5.5. Effect of the Cell's Effort on the Reduction Displacement (Am)

Figure 13 depicts the total displacement vectors of the footing without a cell under dynamic movement. Furthermore, in Figure 14, the effectiveness of the confined sand cell in controlling amplitude reduction in displacement becomes notably more pronounced with increasing cell depth. In contrast, in cases without a cell beneath the footing and with clay soil replaced by compacted sand layers beneath the footing, the decrease in amplitude reduction in displacement occurs at a slower rate as the depth of the sand layers increases. It is evident that surpassing a certain point of cell penetration (Hc/D = 0.50) at Dc/D=1.15 does not yield additional benefits, unlike scenarios without a cell beneath the footing. For instance, at Hc/D = 0.50 and Dc/D=1.15, the amplitude reduction in displacement was 13% with the confined sand cell, whereas in its absence, it increased to 37% for point #1.

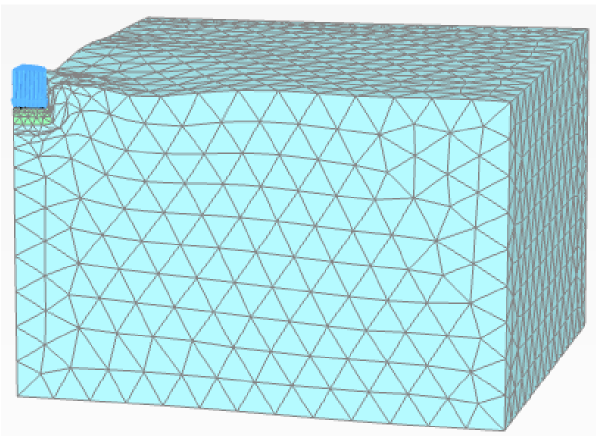

**Figure 13. The total displacement vectors of the footing without a cell under dynamic movement**

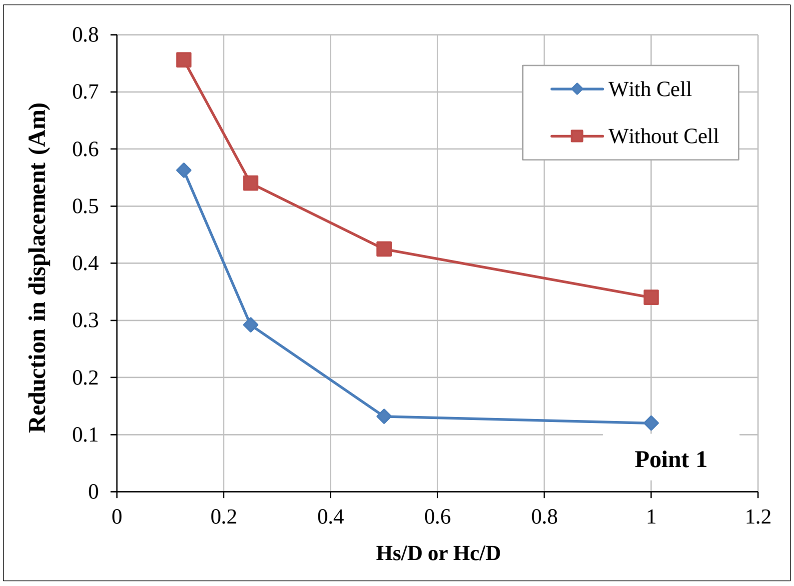


**Figure 14. Variation of Am factor with/without the confined sand cell for point #1 at Dc/D =1.15**

### 5.6. Effect of the Cell's Effort on Am at Different Dynamic Stresses

In Figure 15, the effect of the confined sand cell's efficacy on amplitude reduction (Am) at varying dynamic stresses is detailed. As dynamic stresses fluctuate, the efficiency of the confined sand cell in mitigating amplitude reduction in displacement becomes increasingly apparent. The cell's effectiveness is particularly notable at higher dynamic stresses, where it substantially reduces amplitude reduction compared to cases without cell intervention.

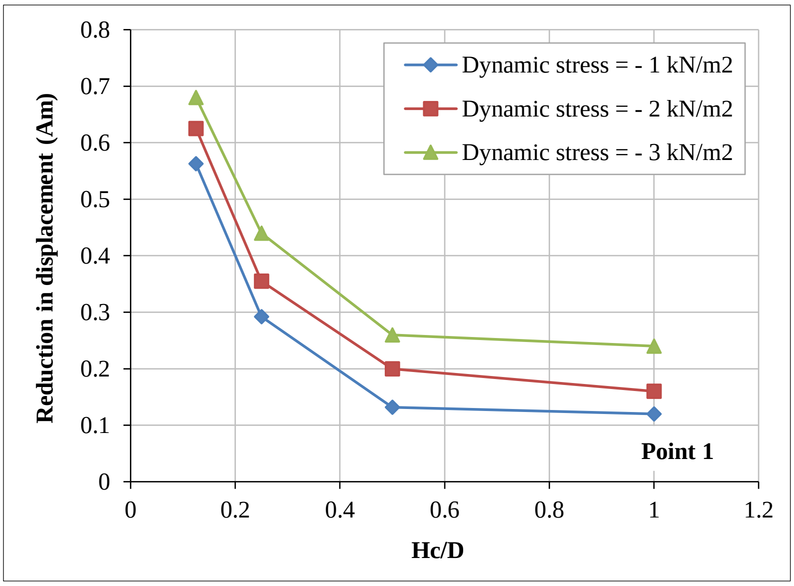


**Figure 15. The variation of the Am factor with normalized cell depth at different dynamic stresses for monitored point #1**

Moreover, detailed analysis reveals that as dynamic stresses increase, the reduction in amplitude is more pronounced at deeper cell depths. This trend underscores the importance of cell depth in optimizing vibration control and minimizing the amplitude reduction factor under varying dynamic loading conditions. Furthermore, comparisons between cases with and without the cell highlight the significant contribution of the confined sand cell to reducing the amplitude reduction factor, particularly at elevated dynamic stresses. This emphasizes the critical role of the cell in enhancing structural resilience and stability under dynamic loading conditions. Overall, Figure 15 provides comprehensive insights into the nuanced effect of the confined sand cell's efforts on amplitude reduction at different dynamic stresses, elucidating its crucial role in vibration control and structural performance optimization. It can be concluded from figure 15 that a range of different dynamic stresses are applied to the footing. Observations reveal that the displacement amplitude increases under a dynamic stress of -3 kN/m$^2$ compared to -1 kN/m$^2$. Throughout various dynamic stresses, the amplitude reduction factor (Am) is notably lower at Hc/D = 0.50 compared to Hc/D = 0.125. Specifically, the figure illustrates that for point #1, at Hc/D = 0.125 and Dc/D = 1.15, the Am increases from 28% to 72% as the dynamic stress escalates from -1 kN/m$^2$ to -3 kN/m$^2$. This highlights the sensitivity of Am to variations in dynamic stresses and the influence of cell depth (Hc/D) on the amplitude reduction factor.

### 5.7. Effect of the Cell's Effort on Am at Different Amplitudes

The impact of the cell's effectiveness on the amplitude reduction factor (Am) varies with different amplitudes, as demonstrated in Figure 16. Upon analysis, it is evident that as the amplitude of displacement increases, so does the amplitude reduction factor (Am). This trend is particularly pronounced when comparing Am at varying amplitudes of dynamic loads. For instance, at lower amplitudes, such as 10, the Am is observed to be relatively lower compared to higher amplitudes, such as 20. This suggests that the cell's efficacy in reducing amplitude is more prominent under higher amplitudes of dynamic loads. Furthermore, the Am is significantly influenced by the depth of the cell (Hc/D). Comparisons between different cell depths reveal varying levels of Am, with shallower depths exhibiting lower Am compared to deeper depths. In summary, Figure 16 illustrates the nuanced effect of the cell's efforts on Am at different amplitudes of dynamic loads, highlighting the importance of considering both the amplitude and depth of the cell in optimizing amplitude reduction. Furthermore, Figure 16 illustrates a range of different amplitudes of dynamic load applied to the footing. It was noted that the displacement amplitude increased with an amplitude of dynamic load of 20 compared to an applied amplitude of dynamic load of 10. Across the various amplitudes of the dynamic load, the amplitude reduction factor (Am) was notably lower at Hc/D = 0.50 compared to Hc/D = 0.125.

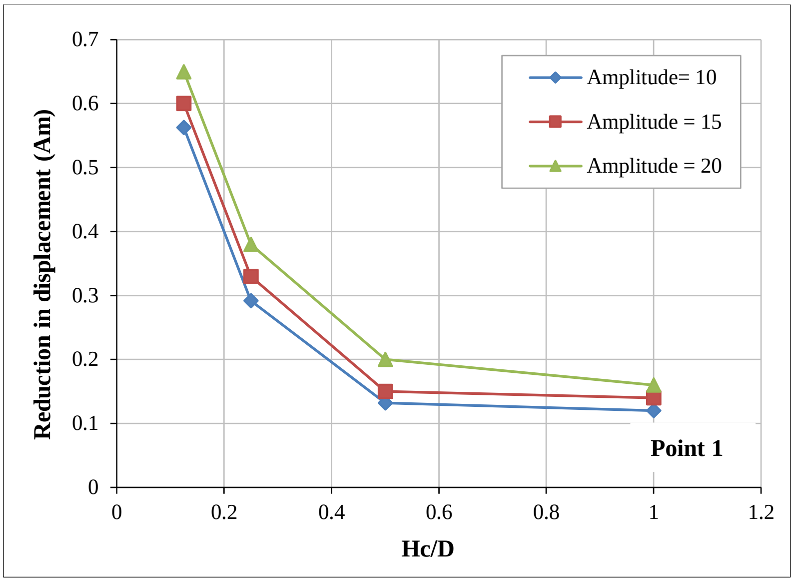


**Figure 16. The variation of the Am factor with normalized cell depth at different amplitudes for monitored point #1**

Specifically, the figure indicates that for point #1, at Hc/D = 0.125 and Dc/D = 1.15, the Am increased from 37.5% to 85.5% as the amplitude of the dynamic load escalated from 10 to 20. This highlights the sensitivity of Am to variations in amplitude and emphasizes the influence of cell depth (Hc/D) on amplitude reduction.

### 5.8. The Load Transfer Mechanism Using Confined Sand Cell

The load transfer mechanism from a machine foundation to a confined sand subgrade with a cell-stabilized medium-stiff clay involves several key processes:

Initial Loading Distribution: When the machine foundation is placed on the ground surface, the initial load is concentrated on the foundation base. The load is transmitted downward through the foundation, generating stress within the underlying soil layers.

Interaction with Confined Sand Subgrade: as the load reaches the confined sand subgrade, the sand material within the cells begins to bear a portion of the load. The confinement provided by the cells prevents lateral spreading of the sand, allowing it to compact and distribute the load evenly over a larger area. The confined sand subgrade acts as a stable platform that supports the machine foundation and reduces the risk of settlement or differential movement.

Stabilization of Medium-Stiff Clay: The presence of the confined cells filled with sand enhances the stability of the surrounding medium-stiff clay soil. The lateral support provided by the confined sand helps to minimize deformations and improve the overall stiffness of the clay soil. This stabilization mechanism prevents excessive settlement or heaving of the clay soil under the machine foundation, ensuring long-term structural integrity.

Load Transfer to Surrounding Soil: Beyond the confined sand subgrade, the load is gradually transferred to the surrounding soil layers, including the medium-stiff clay and any additional soil strata. The load transfer process involves vertical and horizontal stress distributions, with the magnitude of stress decreasing with depth from the foundation base.

Overall Structural Response: the combined effect of the machine foundation, confined sand subgrade, and stabilized clay soil results in a balanced load distribution system. The foundation system remains stable and resilient under dynamic loading conditions, with minimal risk of settlement, differential movement, or structural damage.

By understanding and optimizing the load transfer mechanism from the machine foundation to the confined sand subgrade with cell-stabilized medium-stiff clay, engineers can design robust foundation systems that ensure the long-term performance and stability of civil engineering structures.

### 5.9. Benefits of Confined Sand Cell Stabilization

Improved load distribution: The confined sand cells help distribute the load from the machine foundation more evenly, reducing localized stress concentrations.

Enhanced bearing capacity: By reinforcing the clay soil, the confined cells increase their bearing capacity, allowing them to support heavier loads without excessive settlement.

Reduced settlement: Stabilizing the clay soil with confined cells filled with sand minimizes the risk of settlement under the machine foundation, ensuring long-term stability and structural integrity.

By utilizing confined cells filled with sand to stabilize clay soil under a machine foundation, engineers can effectively enhance the soil's load-bearing capacity, reduce settlement risks, and ensure the long-term stability and performance of the foundation system under dynamic loading conditions. Table 3 shows a comparison between the results of the current study and previous studies.

**Table 3. Comparing the present study to previous studies**

| Study | Previous studies | Methodology | Present study | Comparison / Analysis |
|---|---|---|---|---|
| Ekal & AbidAwn [5] | Examined that reinforcement number of layers affected shallow footing performance under machine foundation loads. | Experimental study | The confined sand cell modelling with different depths | The present study confirms that the percentage of settlement decreases as the depth increases. |
| Won & Langcuyan [14] | Suggested applied the compaction effects on the behaviour of panel-type MSE walls. | Numerical analysis | The soil modelling considered compaction loads typical in actual construction conditions. | The present study extends the importance of compaction effects, which become evident after the application of surcharge load. |
| Azzam [1] | Investigated the effects of increasing the subgrade stiffness using skirts on the foundation subgrade and the structure stability during an earthquake. | Numerical analysis | Using confined sand cells under the foundation at different diameters to increase the subgrade stiffness. | The present study shows that the foundation and the soil within the cell function as a cohesive mass, resulting in progressive densification. As a result, the soil shear strains induced by earthquake loading occur both beneath and outside the densified, treated zone. |
| Azzam [2] | Proposed the use of a confined cell beneath foundations to reduce and manage dynamic effects on sandy subgrades. | Numerical analysis | The novelty of the confined sand cell approach, positioning it as a more targeted, efficient, and cost-effective alternative to existing methods, especially for conditions where large-scale, deep vibrations are a concern. | Present study confirms the importance using confined sand cell to improve the machine foundation behaviour. |

The study introduces a novel approach for vibration mitigation using confined sand cells beneath foundations, a method that offers advantages over traditional techniques commonly used in construction and industrial activities. When compared to existing methods, such as vibration dampers, isolation pads, and passive barriers, the confined sand cell approach stands out for its ability to directly target the source of dynamic forces and control vibration transmission at the foundation level.

***Comparison to Existing Methods:***

Traditional Vibration Dampers: These devices typically absorb or dissipate energy at the surface level, relying on mechanical properties to reduce vibrations. While effective in certain cases, dampers may not provide sufficient control over deep vibrations, particularly in large-scale construction or industrial environments.

Isolation Pads or Mats: These are often used to decouple a structure from the ground and reduce vibration transmission. However, they can be limited in effectiveness, especially for high-frequency vibrations or in situations where high levels of compaction and load are involved.

Passive Barriers: Passive barriers are installed around structures to block or redirect vibrations. These methods work well in some conditions but may not be as effective when the vibration source is deeply embedded in the ground, such as from large generators or heavy machinery.

***Novelty of the Confined Sand Cell Approach:***

The confined sand cell approach differs significantly by focusing on the foundation itself and utilizing the surrounding soil to mitigate vibrations. The cells, filled with compacted sand, act as an integrated system that both absorbs and scatters vibrations, effectively reducing the dynamic response of the soil beneath the structure.

***The Study Highlights the Following Aspects as Novel:***

Confined soil as a dynamic mitigator: By using sand-filled cells with varying diameters and depths, the approach provides a controlled environment for the soil, enhancing its ability to respond to dynamic forces.

Enhanced control over deformation: The confined cells reduce subgrade deformation and displacement amplitude, which traditional methods may not achieve as effectively, particularly for large-scale or industrial activities.

Cost-Effectiveness and efficiency: The use of readily available materials (e.g., sand) within confined cells offers a potentially lower-cost, easily implementable solution compared to other complex mechanical vibration mitigation systems.

The feasibility of confined sand cells in real-world construction depends on several factors. Cost-wise, they may initially be more expensive than traditional methods due to specialized materials and installation processes. Installation is straightforward but requires precision to ensure proper sand compaction and cell integrity. Maintenance is minimal once installed, as sand cells are generally passive structures. However, long-term performance could be influenced by external conditions such as soil compaction and drainage issues, potentially increasing maintenance needs. The technology is most viable in projects where cost flexibility exists or where the sand cells provide clear long-term benefits (e.g., erosion control or load-bearing applications).

In conclusion, the study does effectively highlight the novelty of the confined sand cell approach, positioning it as a more targeted, efficient, and cost-effective alternative to existing methods, especially for conditions where large-scale, deep vibrations are a concern.

## 6. Conclusions

Using Plaxis v2020 software, this study performed a three-dimensional finite element analysis to investigate vibration isolation using a confined sand cell beneath a generator's foundation within an active system. Based on the results obtained, the following conclusions can be drawn:

- The application of a confined sand cell illustrates efficient performance in active isolation settings, effectively managing deformation caused by vibration sources through the interception, scattering, and diffraction of surface waves.
- The confined cell serves as a reinforcement mechanism by offering lateral support to the surrounding clay soil. By filling the confined cell with sand, its capacity to evenly distribute loads and withstand deformations is enhanced. This stabilization approach aims to enhance the overall bearing capacity and stiffness of the clay soil, thereby lowering the potential for settlement and structural damage beneath the equipment foundation.
- An optimal reduction in ground displacement amplitude is achieved with a confined cell depth and diameter of Hc/D = 0.50 and Dc/D = 1.15.
- The introduction of a cell barrier led to a remarkable reduction in total foundation displacement, reaching up to 86% with optimal sand cell geometry.
- Utilizing a confined sand cell can result in the partial to total elimination of displacement in the adjacent free field, thereby improving geometrical damping.
- Under optimal cell geometry conditions, peak particle velocity and excess pore water pressure at point #2 in the free field are reduced by 62% and 87%, respectively, with Dc/D=1.15 and Hc/D=0.50 compared to their initial values.
- The depth of the cell (Hc/D) exerts a significant influence on the amplitude reduction factor (Am). Comparative analysis across different cell depths demonstrates that shallower depths exhibit higher Am values compared to deeper depths.
- It is noteworthy that at point #1, with a depth ratio of Hc/D = 0.125 and a normalized cell diameter (Dc/D) of 1.15, the amplitude reduction factor (Am) increases significantly from 37.5% to 85.5% as the amplitude of the dynamic load increases from 10 to 20.

## 7. Declarations

### 7.1. Author Contributions

Conceptualization, E.K. and W.A.; methodology, W.A. and E.K.; software, E.K.; validation, E.K., W.A., and M.E.; formal analysis, E.K.; investigation, E.K.; resources, W.A.; data curation, E.K.; writing—original draft preparation, E.K.; writing—review and editing, M.E.; visualization, W.A.; supervision, W.A. All authors have read and agreed to the published version of the manuscript.

### 7.2. Data Availability Statement

The data presented in this study are available on request from the corresponding author.

### 7.3. Funding

The authors received no financial support for the research, authorship, and/or publication of this article.

### 7.4. Conflicts of Interest

The authors declare no conflict of interest.

## 8. References

[1] Azzam, W. R. (2014). Seismic response of bucket foundation and structure under earthquake loading. Electronic Journal of Geotechnical Engineering, 19, 1477-1489.

[2] Azzam, W. R. (2015). Utilization of the confined cell for improving the machine foundation behavior-numerical study. Journal of GeoEngineering, 10(1), 17–23. doi:10.6310/jog.2015.10(1).3.

[3] Khalil, M. M. (2023). Dynamic Response of Machine Foundations Supported on Rigid Inclusions. Proceedings of the 4th International Conference on Civil Engineering Fundamentals and Applications (ICCEFA 2023), Lisbon, Portugal. doi:10.11159/iccefa23.112.

[4] Liu, L., Zhao, J., Liu, X., & Lv, S. (2023). Dynamic characteristics and reinforcement mechanism of silty soil improved by regenerated fiber polymer. Scientific Reports, 13(1), 1–13. doi:10.1038/s41598-023-45281-2.

[5] Ekal, S. A., & H. AbidAwn, S. (2024). A Study of the Effect of Reinforcement Layers on the Performance of Shallow Footing Under Machine Foundation Loads. Bilad Alrafidain Journal for Engineering Science and Technology, 3(2), 73–84. doi:10.56990/bajest/2024.030207.

[6] Tang, X., & Chen, P. (2024). Combined Earthquake- Wave Effects on the Dynamic Response of Long- Span Cable- Stayed Bridges. Advances in Civil Engineering, 6109335. doi:10.1155/2024/6109335.

[7] Kennedy, C. (2024). The Effect of Dynamic Response Characteristics in Different Confining Pressures of Damping Ratio and Shear Modulus of Sandy Soil. Research Square (Preprint), 1-21. doi:10.21203/rs.3.rs-4436233/v1.

[8] Akpan, W. A., Orazulume, C. M., & Nyaudo, G. E. I. Dynamic Response Studies of Machine Tools Foundation: Critical Analytic Models Versus ANN. International Journal of Research in Engineering and Science (IJRES), 12(11), 1-17.

[9] Bazoobandi, S., Shamekhi Amiri, M., & Keramati, M. (2024). Laboratory Evaluation of Vibration Isolation of Dynamic Loads Caused by Machine Foundations by Surface Trenches. Shock and Vibration, 9215081, 1–16. doi:10.1155/2024/9215081.

[10] Likitlersuang, S., Chheng, C., Surarak, C., & Balasubramaniam, A. (2018). Strength and stiffness parameters of Bangkok clays for finite element analysis. Geotechnical Engineering Journal of the SEAGS & AGSSEA, 49(2), 150-156.

[11] Bentley Systems. (2020). PLAXIS 3D - Tutorial Manual. Bentley Systems, Pennsylvania, United States.

[12] Allawi, A. A., & S. Mohammed, Q. (2022). Numerical analysis of a concrete foundation under a combination of a dynamic and a seismic load. Journal of Engineering, 28(2), 18–39. doi:10.31026/j.eng.2022.02.02.

[13] Basha, A., Azzam, W., & Elsiragy, M. (2024). Utilization of Sand Cushion for Stabilization of Peat Layer Considering Dynamic Response of Compaction. Civil Engineering Journal (Iran), 10(4), 1182–1195. doi:10.28991/CEJ-2024-010-04-011.

[14] Won, M. S., & Langcuyan, C. P. (2020). A 3D numerical analysis of the compaction effects on the behavior of panel-type MSE walls. Open Geosciences, 12(1), 1704–1724. doi:10.1515/geo-2020-0192.

[15] Mirmoradi, S. H., & Ehrlich, M. (2018). Numerical simulation of compaction-induced stress for the analysis of RS walls under working conditions. Geotextiles and Geomembranes, 46(3), 354–365. doi:10.1016/j.geotexmem.2018.01.006.

[16] Cui, K., Défossez, P., & Richard, G. (2007). A new approach for modelling vertical stress distribution at the soil/tyre interface to predict the compaction of cultivated soils by using the PLAXIS code. Soil and Tillage Research, 95(1–2), 277–287. doi:10.1016/j.still.2007.01.010.

[17] Mirmoradi, S. H., & Ehrlich, M. (2014). Modeling of the compaction-induced stresses in numerical analyses of GRS walls. International Journal of Computational Methods, 11(2), 1342002. doi:10.1142/S0219876213420024.

[18] Woods, R. D. (1968). Screening of Surface Wave in Soils. Journal of the Soil Mechanics and Foundations Division, 94(4), 951–979. doi:10.1061/jsfeaq.0001180.

[19] Aminfar, M. H., Azar, B. F., Ebadi, H., & Ahmadi, H. (2009). Change of pore water pressure inside the foundation of Alavian earthfill dam, Iran: A comparison between observed and predicted values. Journal of Applied Sciences, 9(8), 1489–1495. doi:10.3923/jas.2009.1489.1495.

[20] Finno, R. J., & Zapata-Medina, D. G. (2014). Effects of Construction-Induced Stresses on Dynamic Soil Parameters of Bootlegger Cove Clays. Journal of Geotechnical and Geoenvironmental Engineering, 140(4), 1–12. doi:10.1061/(asce)gt.1943-5606.0001072.

[21] Akan, R., & Sert, S. (2021). Investigation of the Consolidation Behavior of Soft Soil Improved with Vertical Drains by Finite Element Method. International Journal of Engineering and Applied Sciences, 13(3), 93–105. doi:10.24107/ijeas.1002115.